Supporting information

Zeolite Growth by Synergy Between Solution-mediated and Solid-phase Transformations

Manh Huy Do[a,c], Tuo Wang[b], Dang-guo Cheng[*a], Fengqiu Chen[a], Xiaoli Zhan[a], and Jinlong Gong[*b]

[a]*Key Laboratory of Biomass Chemical Engineering of Ministry of Education, Department of Chemical and Biological Engineering, Zhejiang University, Hangzhou 310027, Zhejiang, China*

[b]*Key Laboratory for Green Chemical Technology of Ministry of Education, School of Chemical Engineering and Technology, Tianjin University; Collaborative Innovation Center of Chemical Science and Engineering, Tianjin 300072, China.*

[c]*Institute of Chemical Technology, Vietnamese Academy of Science and Technology, 01 Mac Dinh Chi, District 1, Ho Chi Minh, Vietnam*

*Corresponding author: dgcheng@zju.edu.cn; jlgong@tju.edu.cn

Figure S1. Photographs (a) of the hydrogel before and after adding sodium hydroxide with its schematic structure, (b) of the monolith samples collected after various reaction times of the hydrothermal treatment of the quasi-solid gel at 175 °C.

.

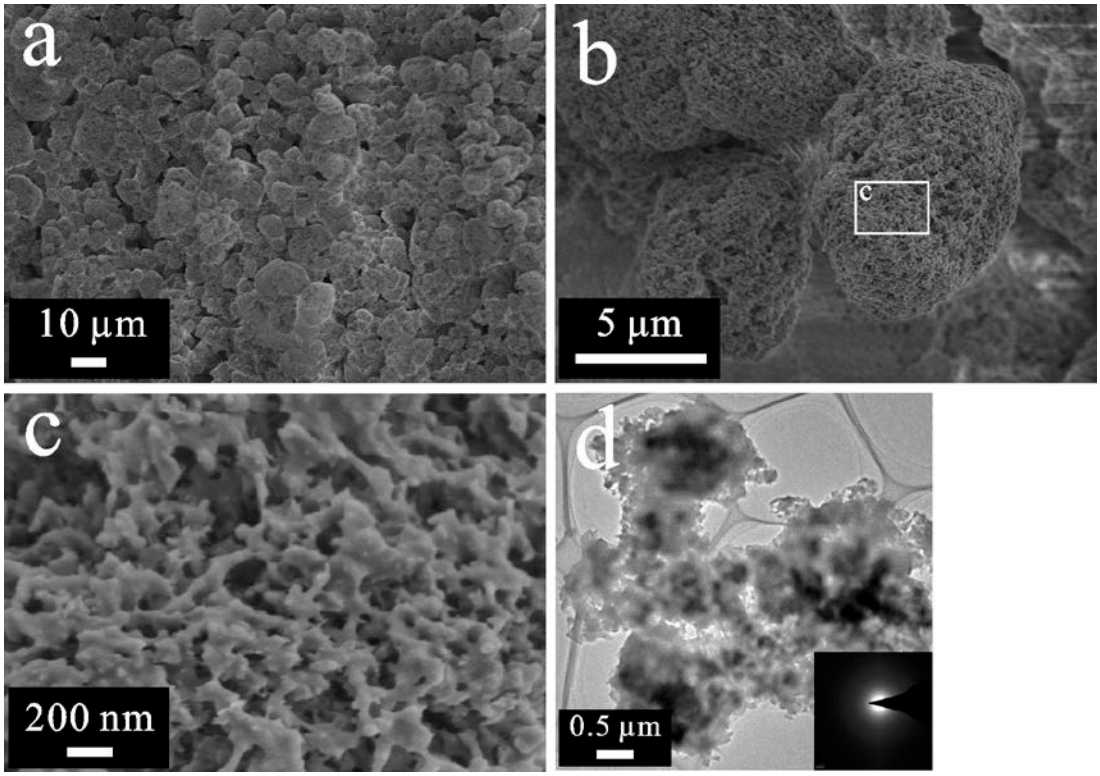

Figure S2. SEM (a-c) and TEM (d) images of the monolith sample obtained after the hydrothermal treatment for 10 min at 175 °C. Representative electron diffraction pattern (inset in d) confirm the amorphous nature of the gel aggregates.

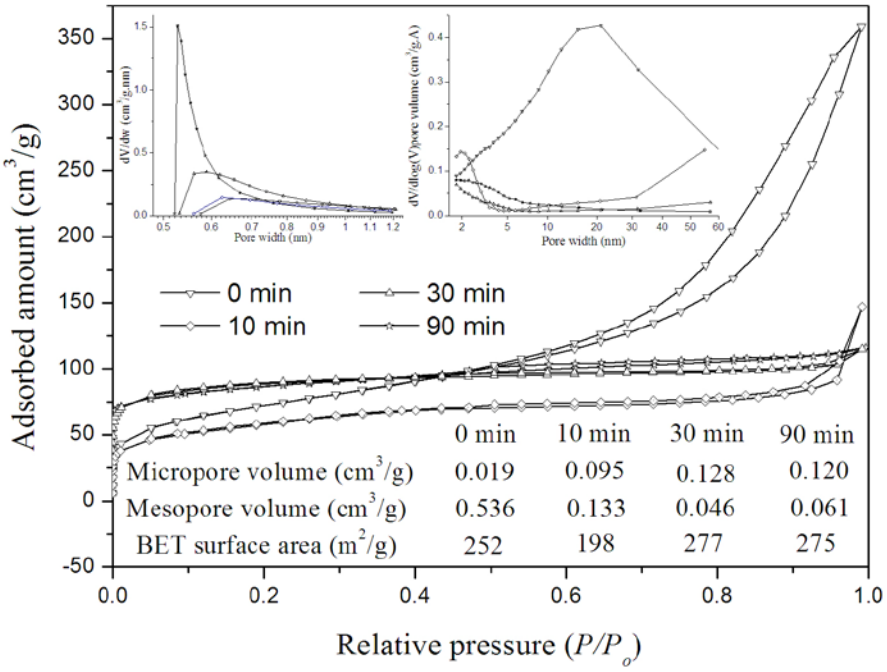

Figure S3. Nitrogen adsorption–desorption isotherms of the quasi-solid gel and monolith sample collected after various times of the hydrothermal treatment at 175 °C. The micro- mesopore-size distributions and textural data (micro- mesopore volumes and BET surface area) are given in the insets. The mesopore volume and BET surface area of the monolith material after 10 min of the hydrothermal treatment are smaller than those of the initial gel, reflecting the loss of mesoporosity resulted from increase in the polymerization rate. The micropores with size of about 0.55 nm, typical for micropores associated with 10-ring channels of the MFI type zeolite were observed after 30 min of the hydrothermal treatment.

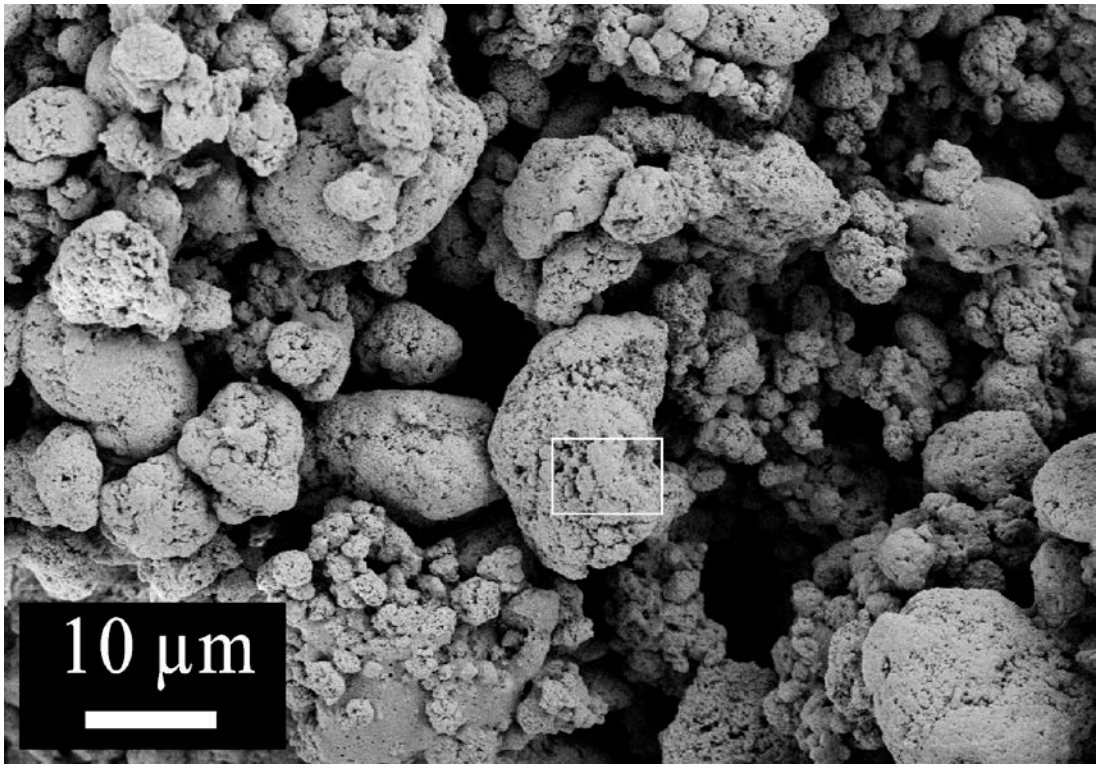

Figure S4. SEM images of the monolith sample collected after 30 min of the hydrothermal treatment at 175 °C. The region highlighted by a rectangle is shown magnified in Figure 2a.

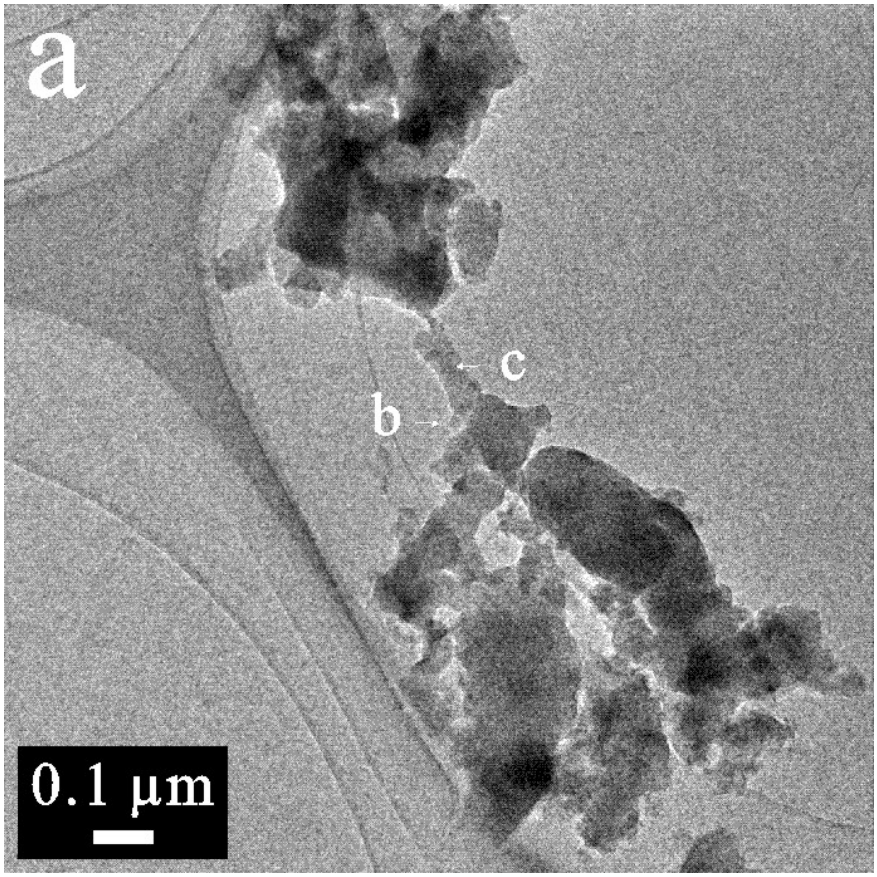

Figure S5. a-c) TEM images of the monolith sample collected after 30 min of the hydrothermal treatment at 175 °C. b-d) HRTEM images of the equilibrated gel phase, showing the presence of several hundred 10-member ring (10-MR) pores of the MFI type framework structure. The regions marked by squares in (b, d) with corresponding FFTs (insets) showing the ordered regions of the MFI type framework structure. Arrowhead in FFT 2 (inset in b) indicated a spot corresponding to d_{hkl}=0.96 nm, which can be $d_{[200] \text{ or } [111]}$ of the MFI framework structure. The 1 nm spaced lattice fringes only about 2 nm in length formed by the arrangement of the 10-MR channels can easy be observed in (c). The lattice fringes with a spacing of about 0.2 nm formed by the arrangement of the 10, 6 and 5-MR pores also be indicated in (d). The inset FFT, taken from the whole image d), shows diffuse rings corresponding to d spacings of 0.635, 0.435, 0.384 and 0.200 nm, which are consistent with the (102), (013), (501) and (1000) reflections of the MFI zeolite structure. Reflections with d_{hkl} at low 2θ region did not exhibited distinctly may be due to short ordered arrange of 10-MR pores. Projection of the MFI framework structure down the [010] direction (inset in d) showing the arrangement of the 10, 6, and 5-MR pores.

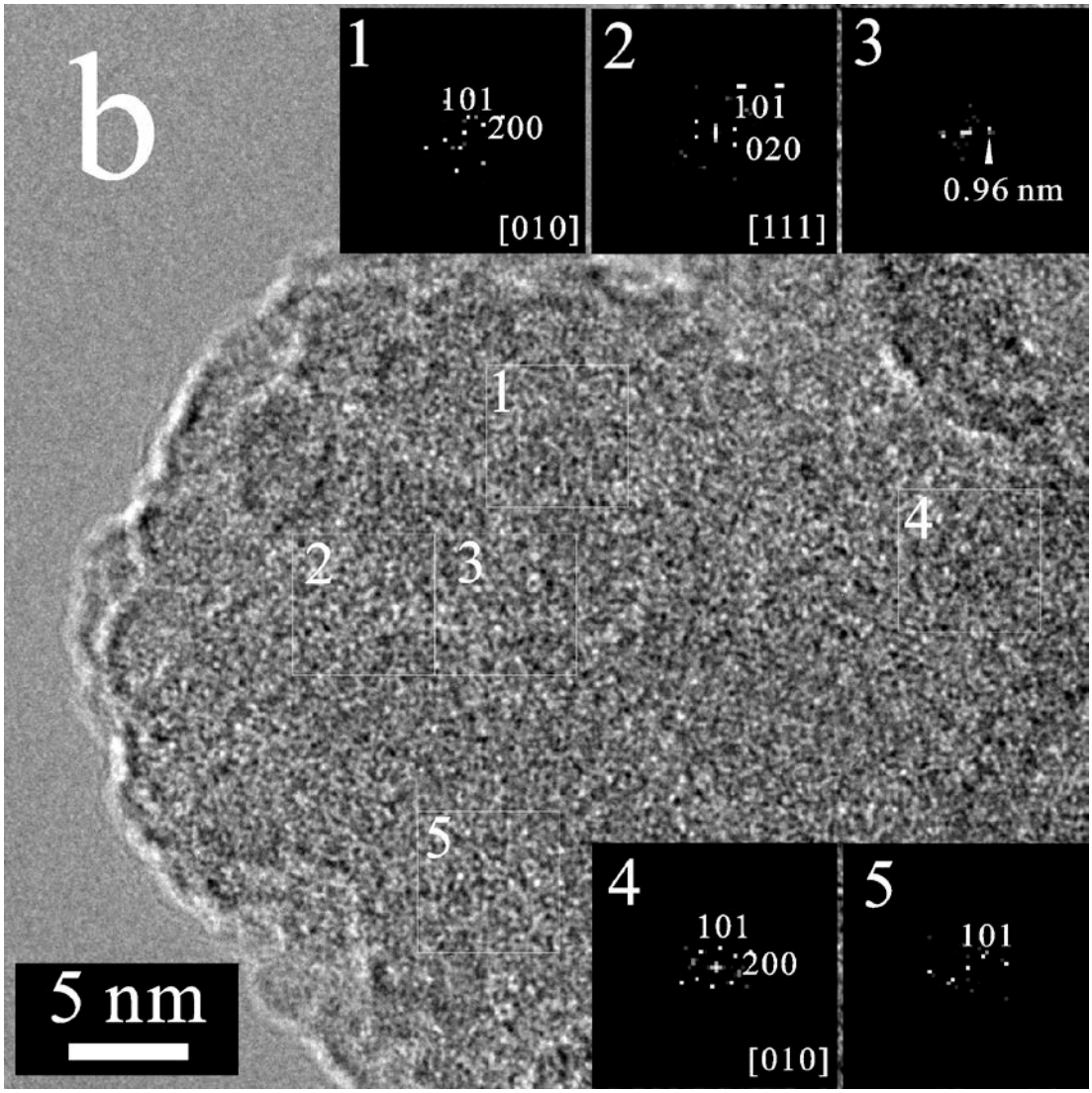

Figure S5

(Cont.)

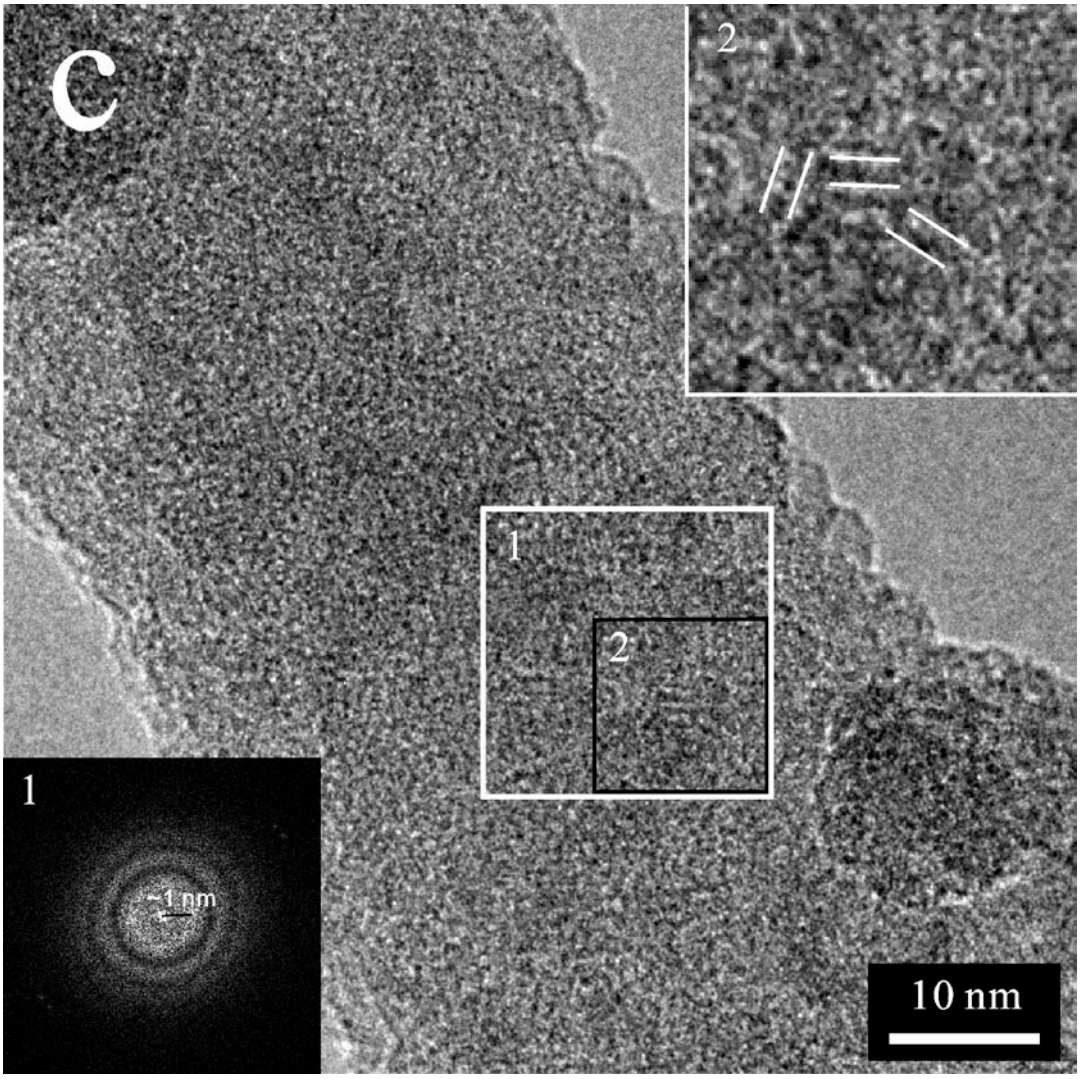

Figure S5 (Cont.)

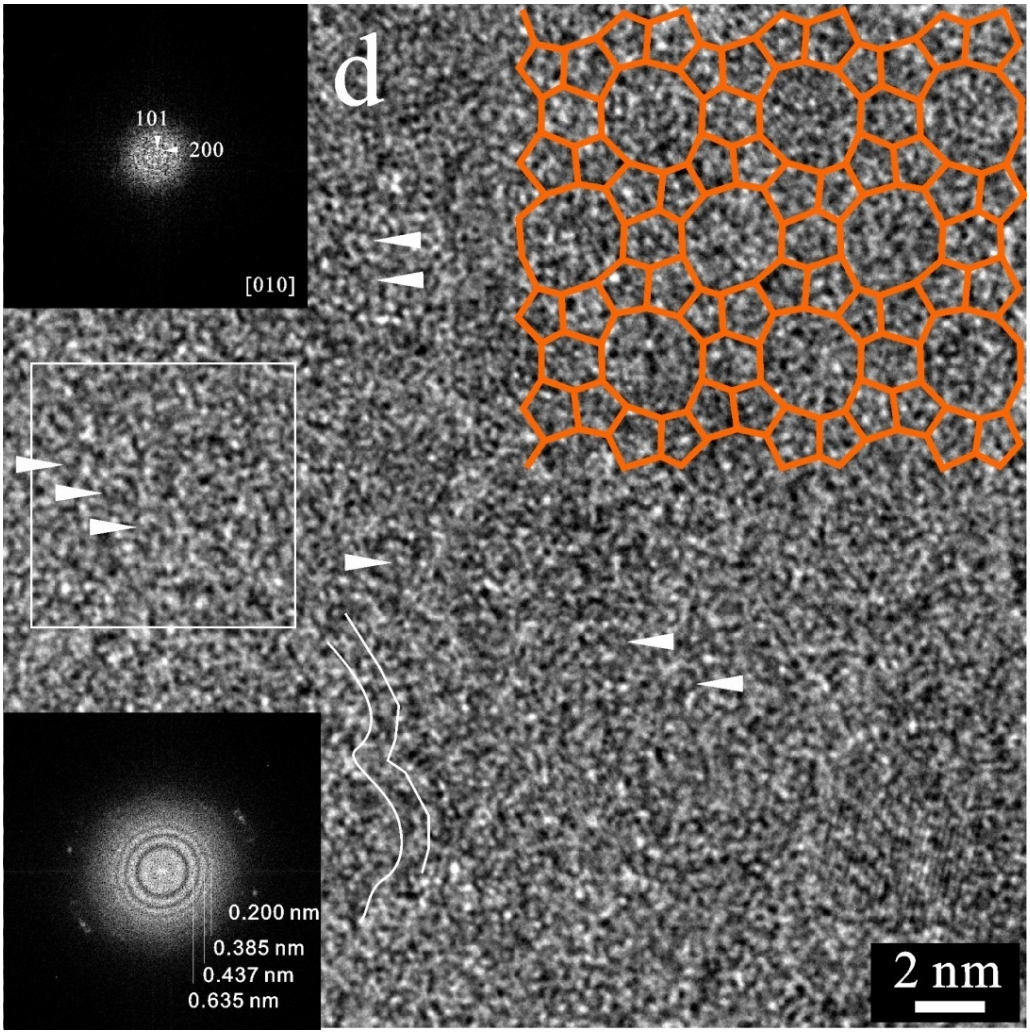

Figure S5

(Cont.)

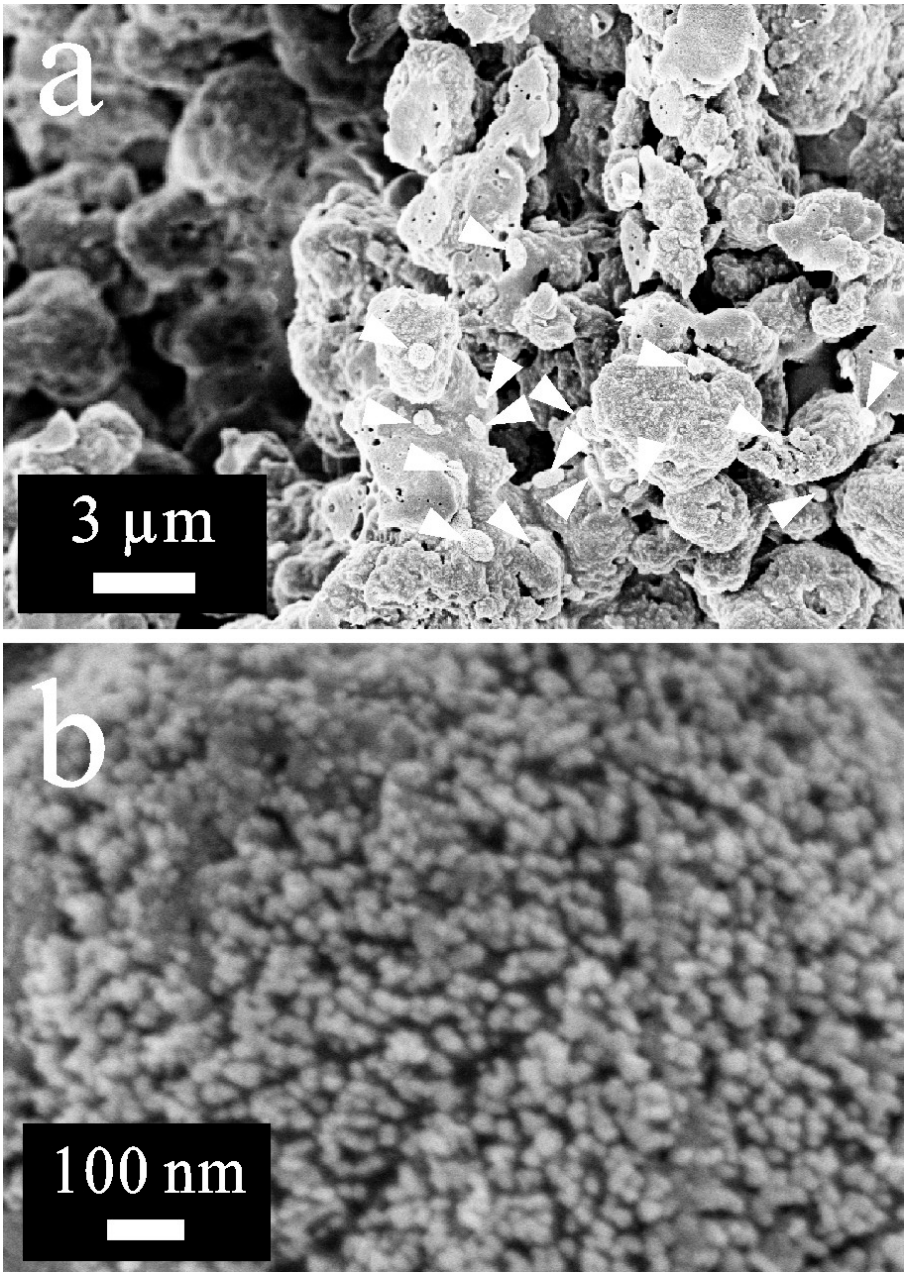

Figure S6. SEM images of the sample collected after 1 hour of the hydrothermal treatment at 175 °C. Arrowheads in (a) mark coffin shaped aggregates formed by attachment of nascent crystals and 10-50 nm polycrystal particles on the equilibrated gel phase. b) HRSEM of a coffin shaped aggregate in (a).

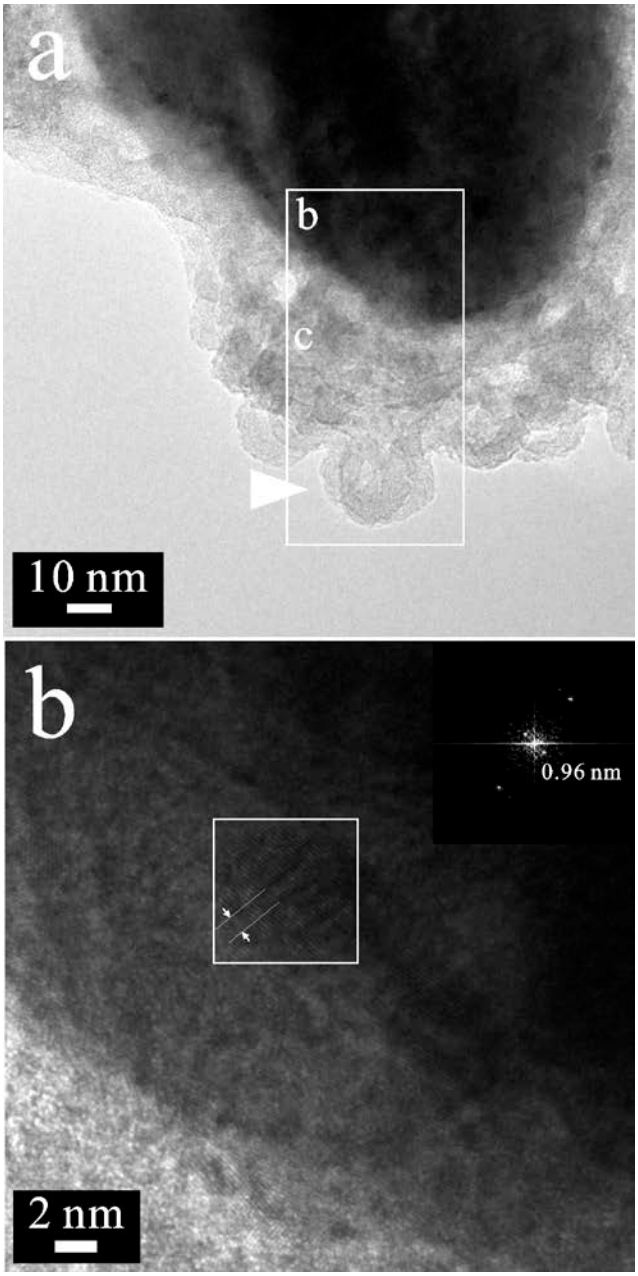

Figure S7. a) TEM image of a coffin shaped aggregate after 1 hour. Arrowhead shown a polycrystal aggregate is shown magnified in Fig. 2d. b) HRTEM image of (a) shows the lattice fringes with spacing of 0.96 nm (the spacing also is indicated by inset FFT) corresponding to $d_{[200] \text{ or } [111]}$ of the MFI framework structure. c) HRTEM image of (a) showing the attached nascent crystals on the aggregate surface. Arrowheads mark the 10-MR channels along the *b* axis. The FFT insets from the numbered regions show spots corresponding to d spacings of 1.23 and 0.96 nm, which can be $d_{[101]}$ and $d_{[200] \text{ or } [111]}$ of the MFI framework structure.

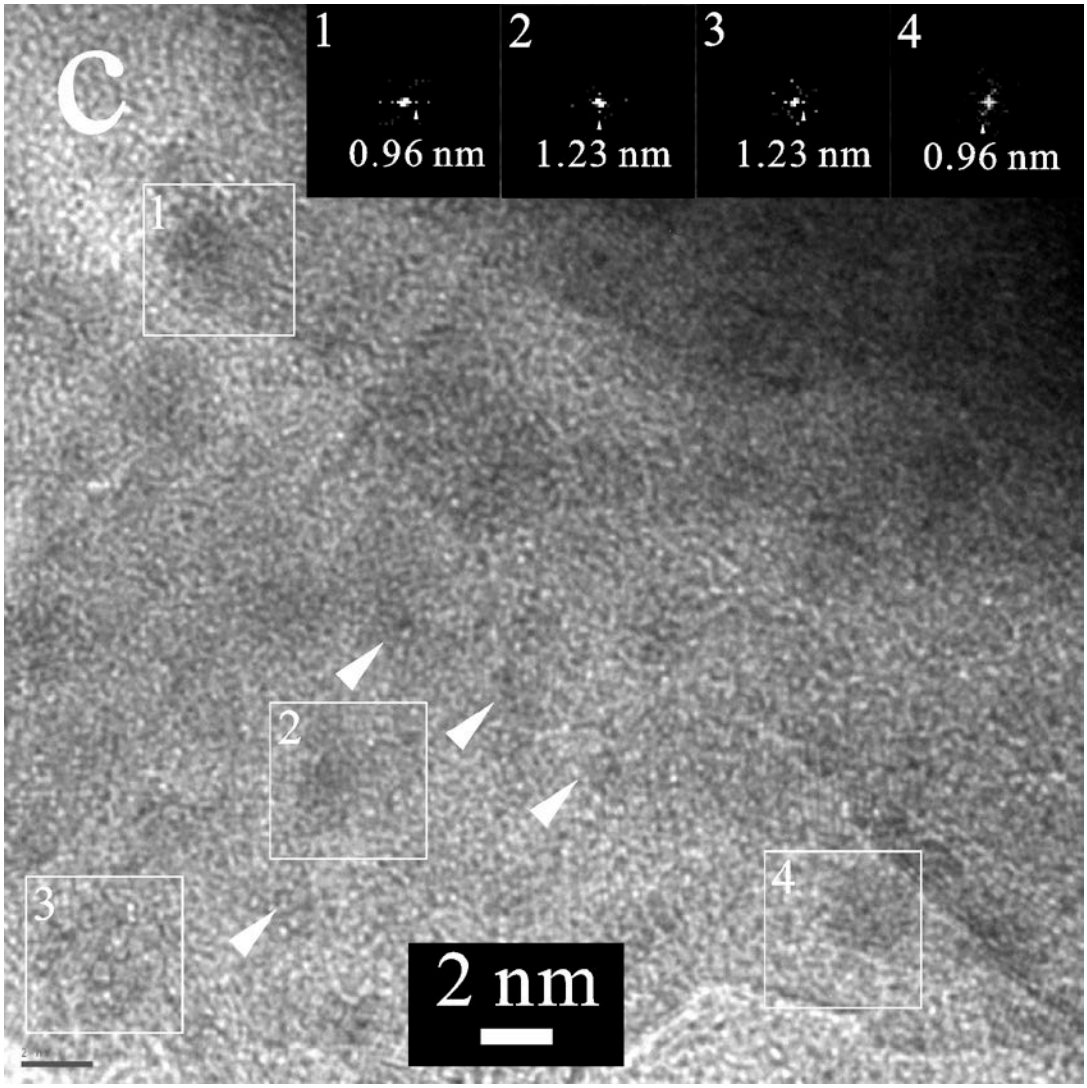

Figure S7

(Cont.)

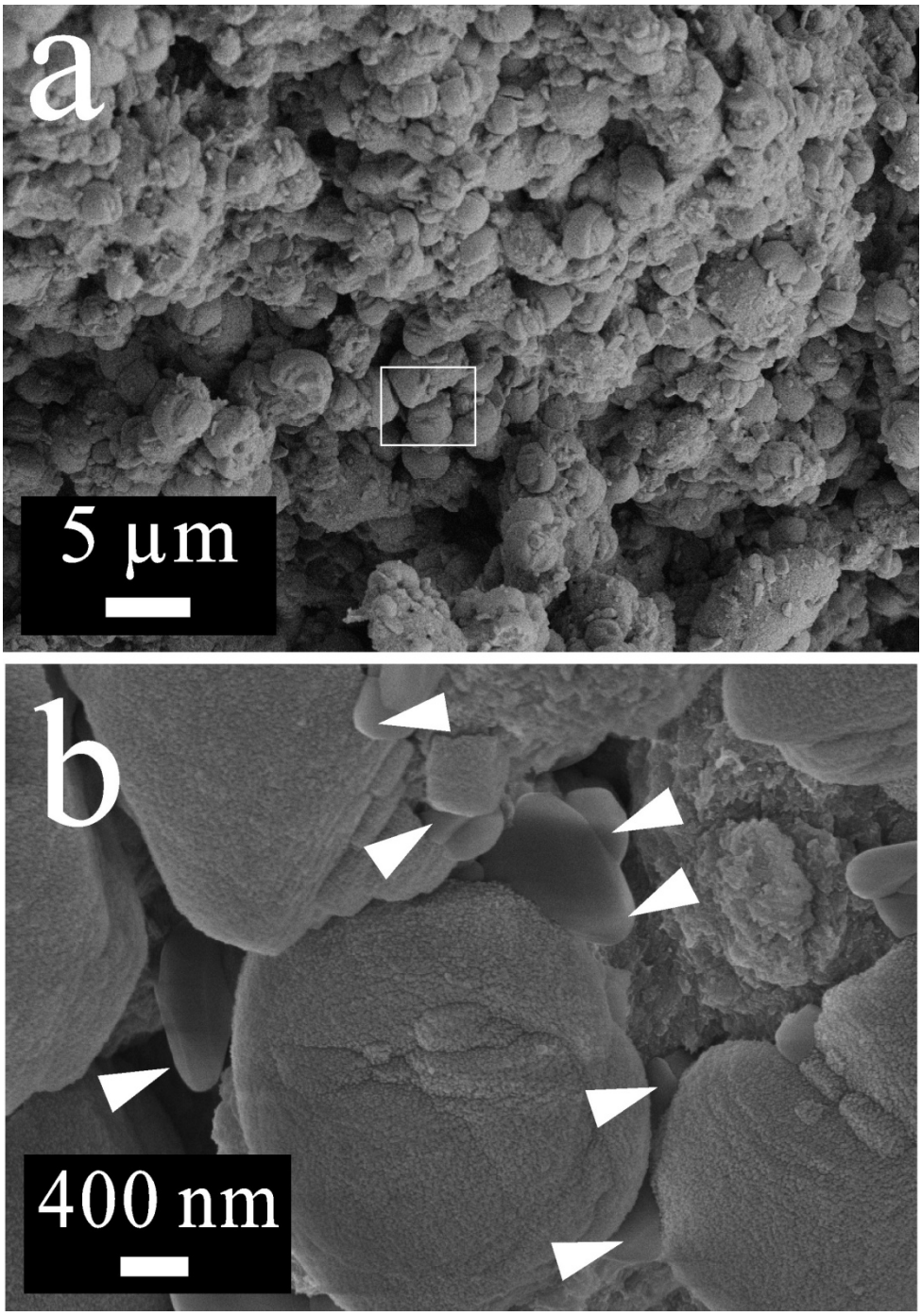

Figure S8. SEM images of the monolith sample collected after 1.5 hours of the hydrothermal treatment at 175 °C. Arrowheads in (b) highlight the equilibrated gel phase of the condensed primary aggregates.

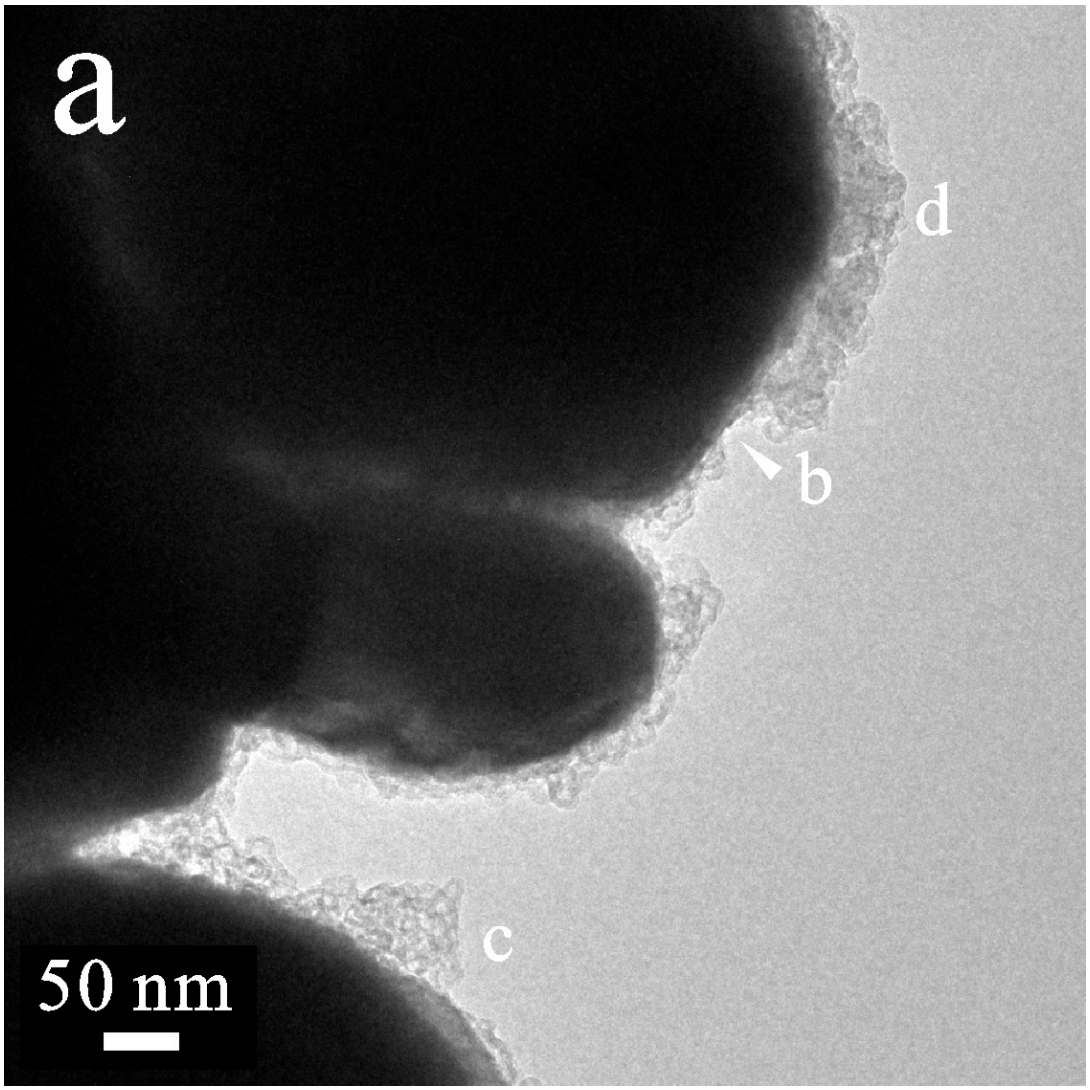

Figure S9. TEM images of the monolith sample collected after 1.5 hours of the hydrothermal treatment at 175 °C. Arrows in (b) indicate the insertion of the polycrystal particles which can be formed at the 1 h stage. c) HRTEM image of the polycrystal aggregate in a) with FFT inset from the square region showing forward coalescence into the single MFI crystal with creasing [010] crystal habit. d) HRTEM image of (a), showing the coalescence of the crystals along [100] direction and the orientated attachment of the zeolite nuclei at the [100]+[101] edge angles. e) A partial single MFI crystal introduced into the surface of the coffin shaped particle, confirming the zeolite crystal growth occurs at the liquid-solid interface of the condensed primary aggregates..

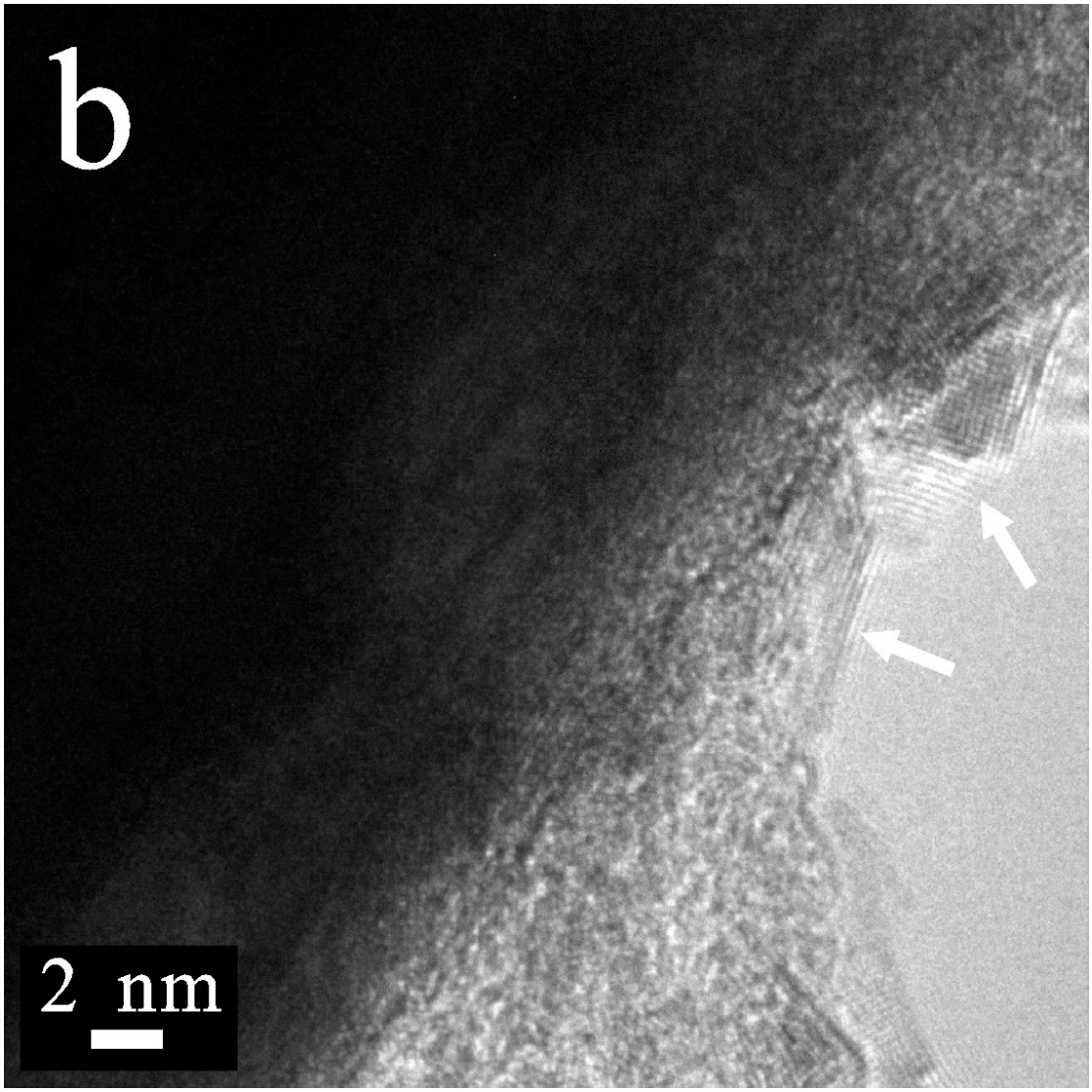

Figure S9

(Cont.)

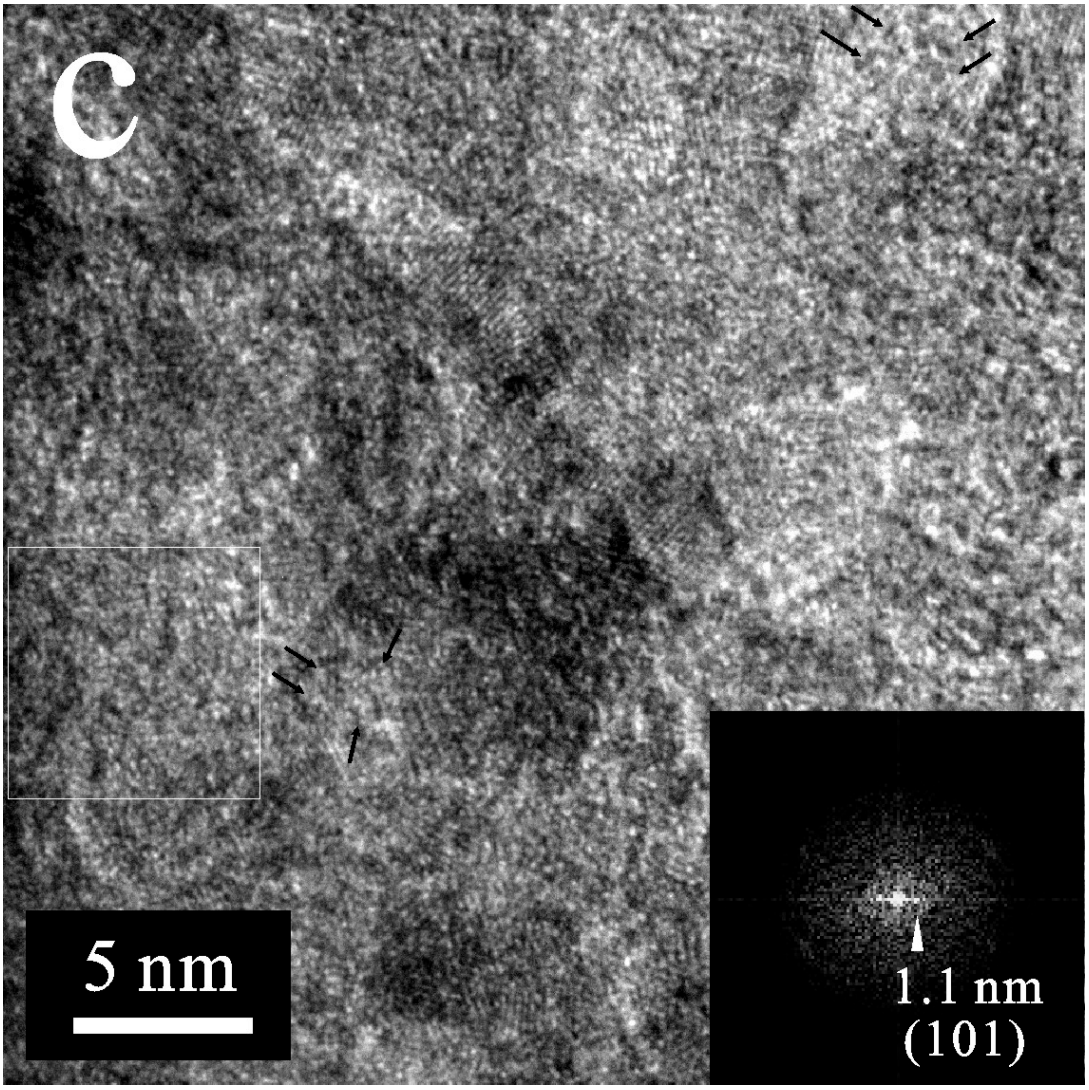

Figure S9

(Cont.)

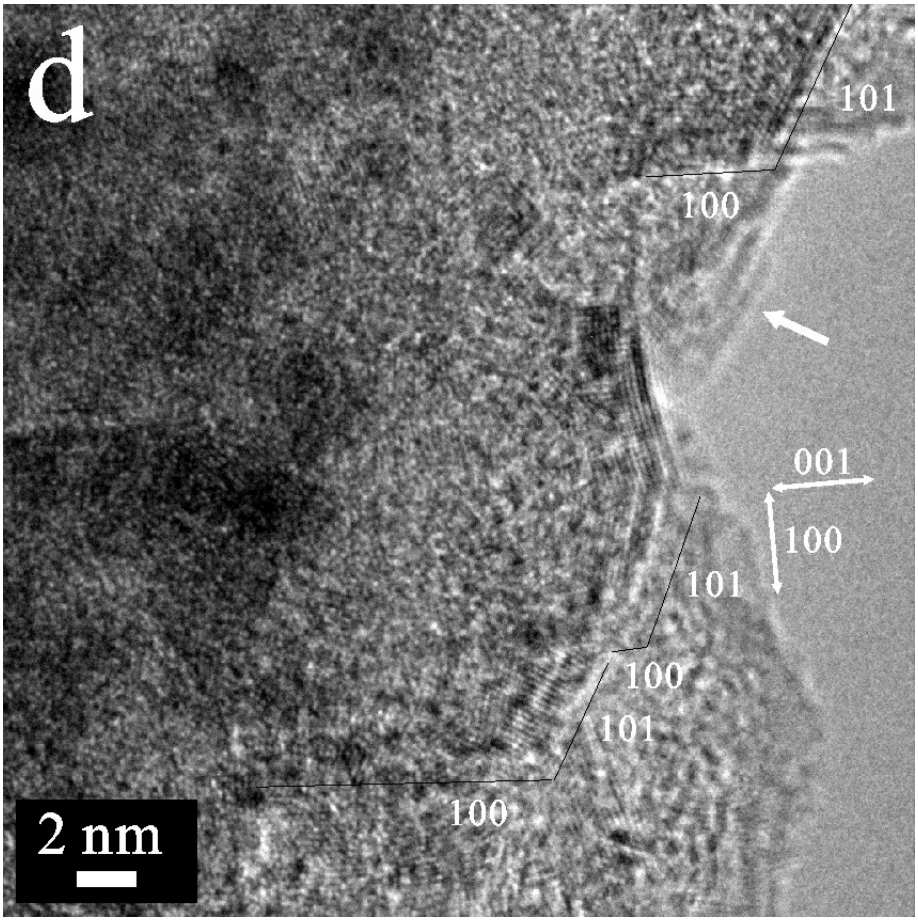

Figure S9

(Cont.)

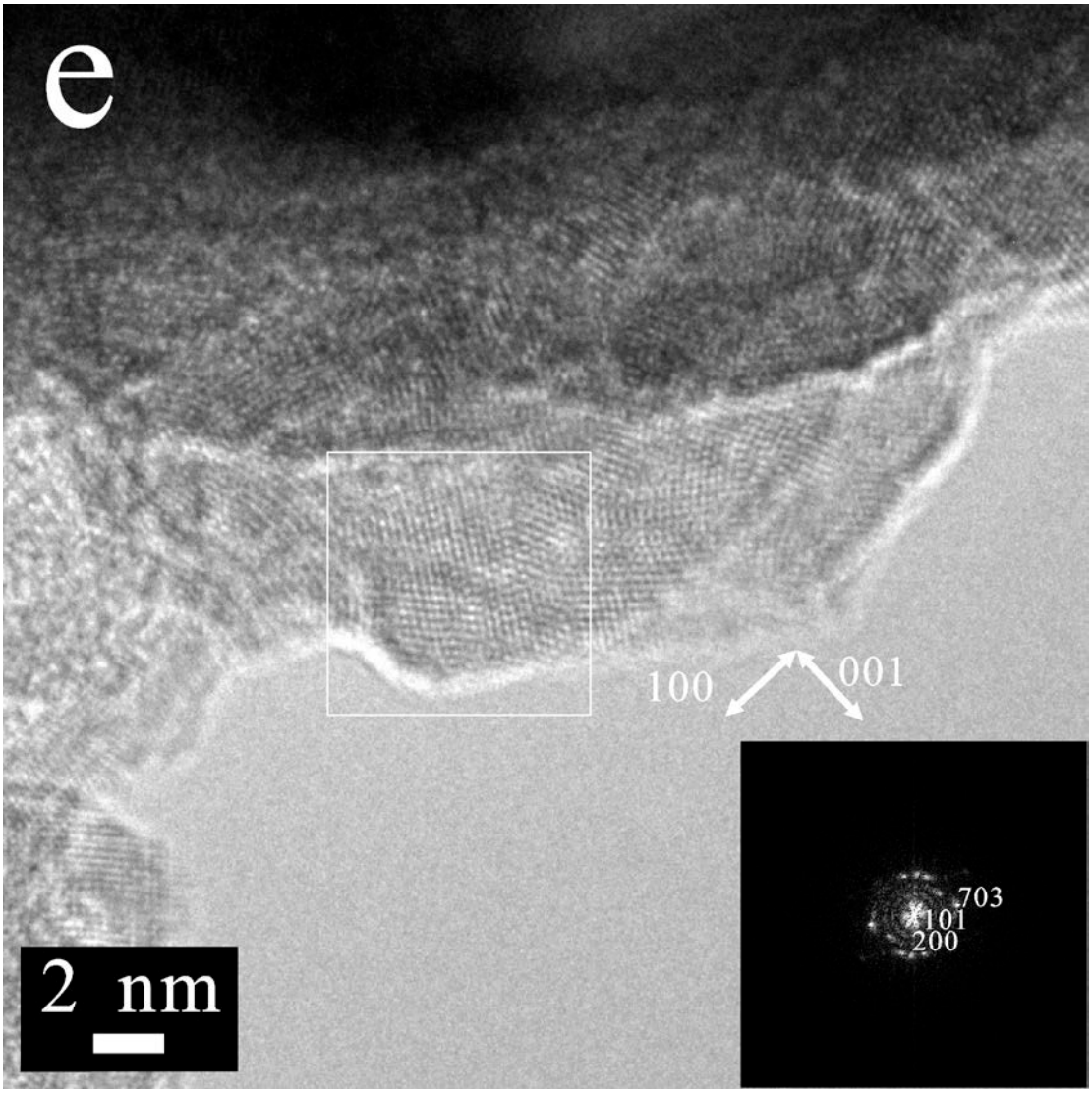

Figure S9

(Cont.)

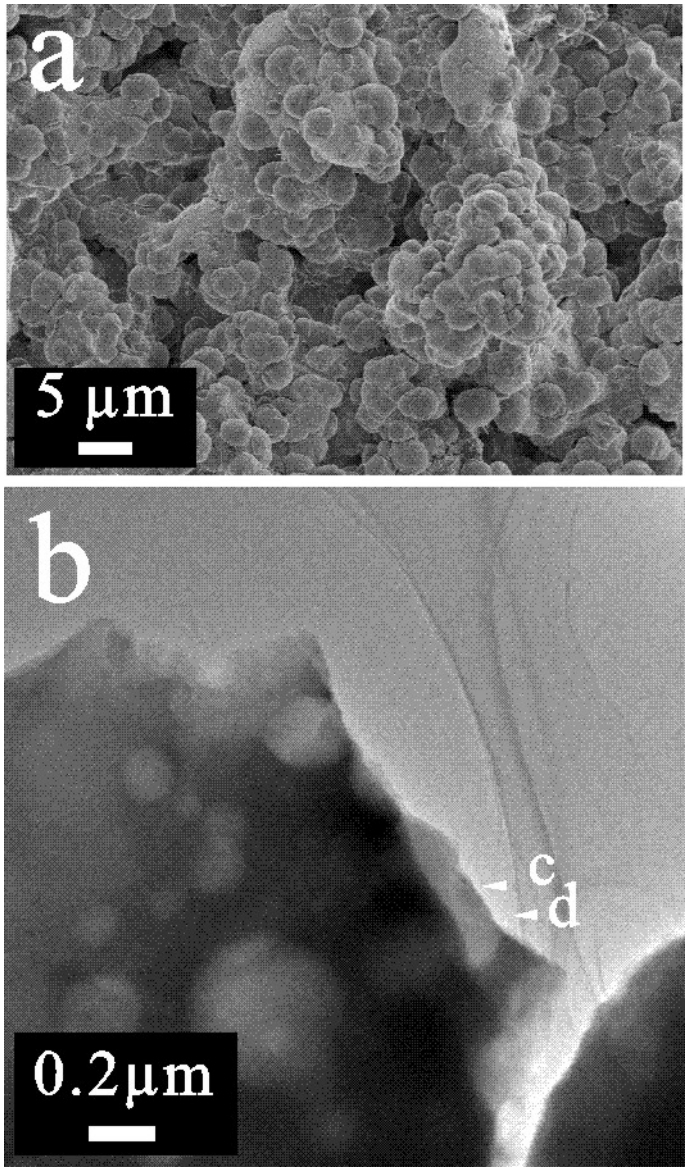

Figure S10. SEM (a) and TEM (b-f) images of the monolith sample collected after 2 hours of the hydrothermal treatment at 175 °C. HRTEMs (c-f) show the edge dislocations (c, e) formed due to imperfectly oriented aggregation and the single crystal domains (d, f) after coalescence.

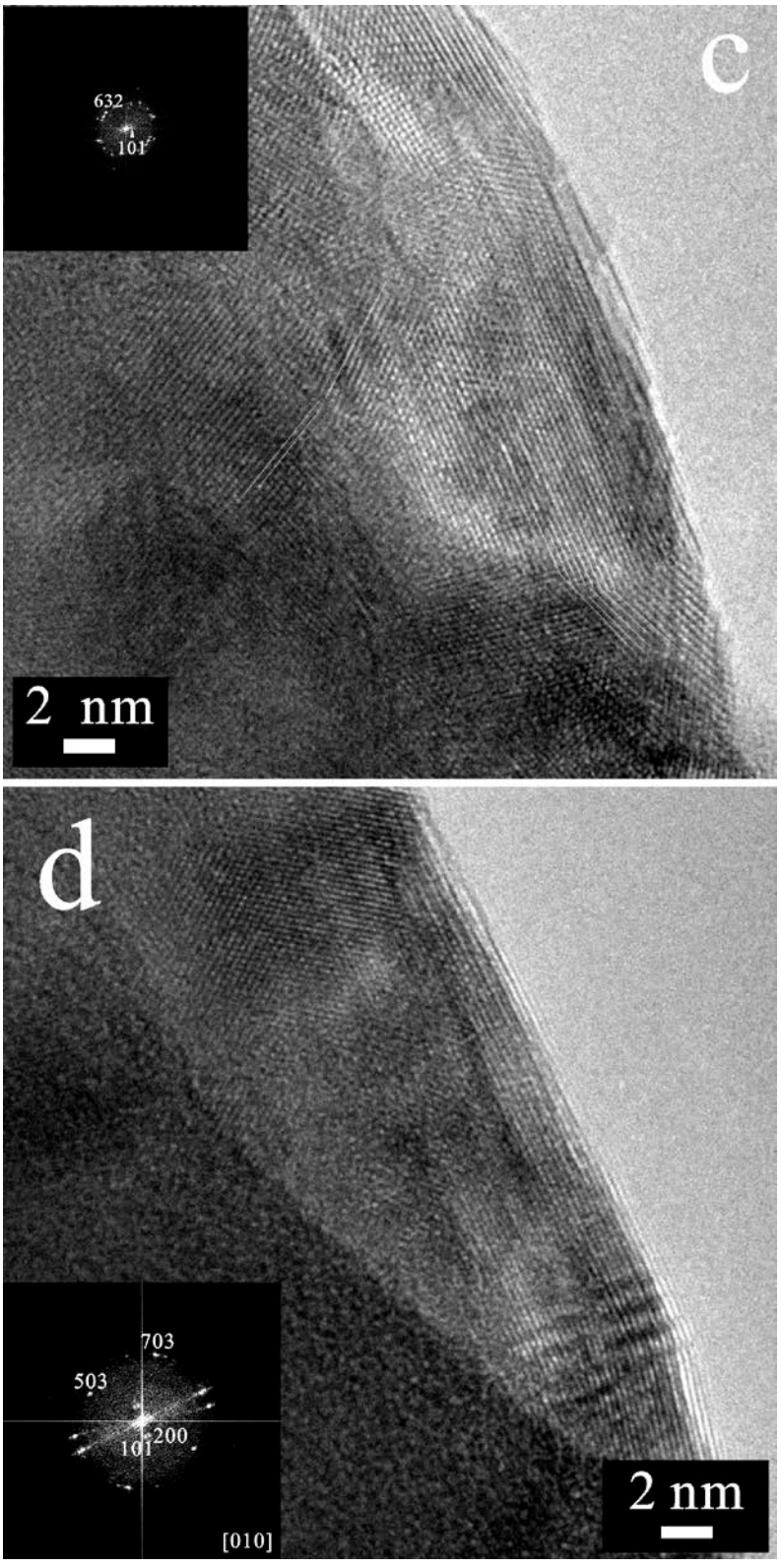

Figure S10 (Cont.)

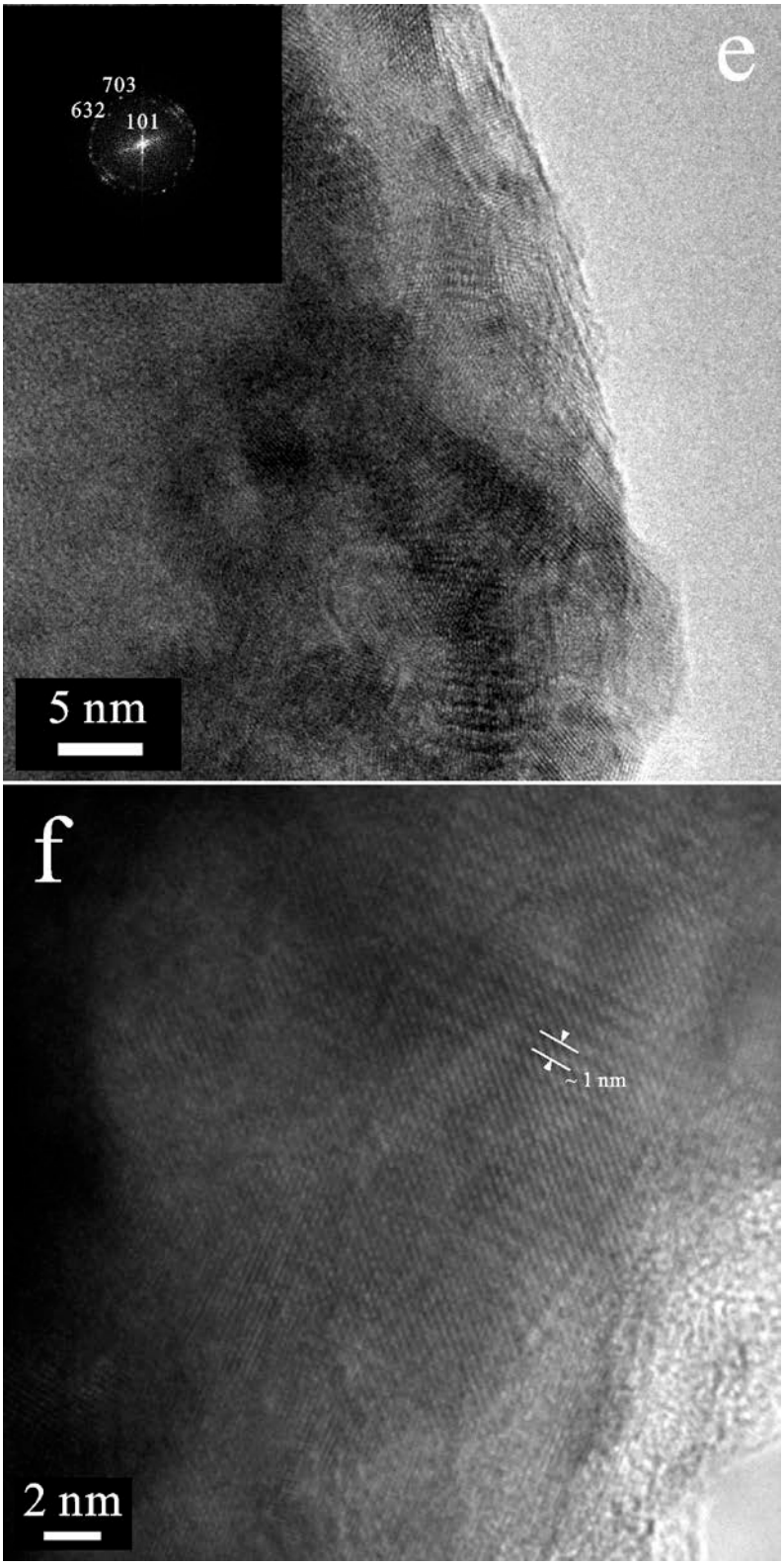

Figure S10 (Cont.)

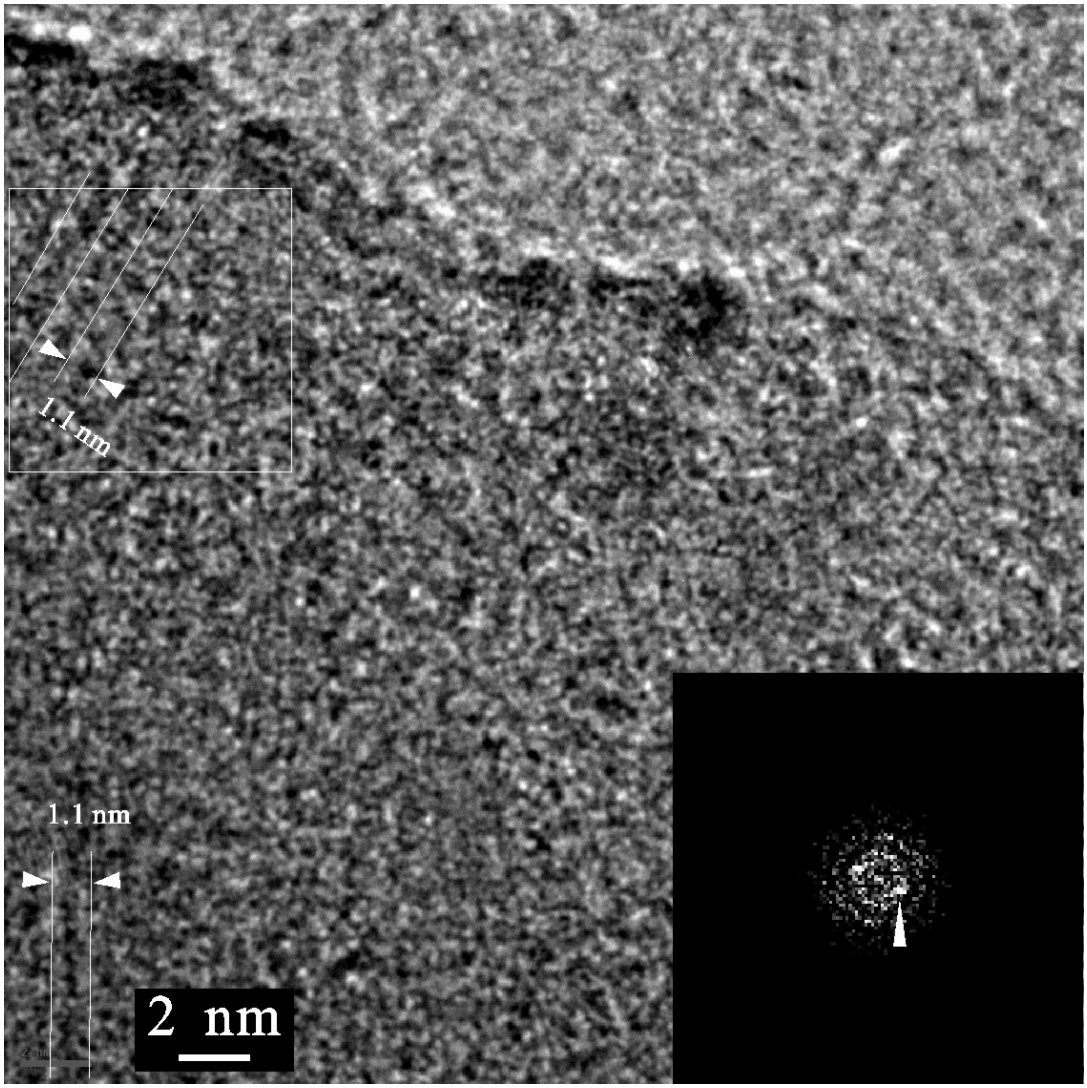

Figure S11. HRTEM images of Figure 3 showing the local order of 10-MR channel of the MFI framework. Arrowhead in inset FFT from the square region indicated a spot corresponding to d_{hkl}=1.1 nm, which can be $d_{[101]}$ of the MFI framework structure.

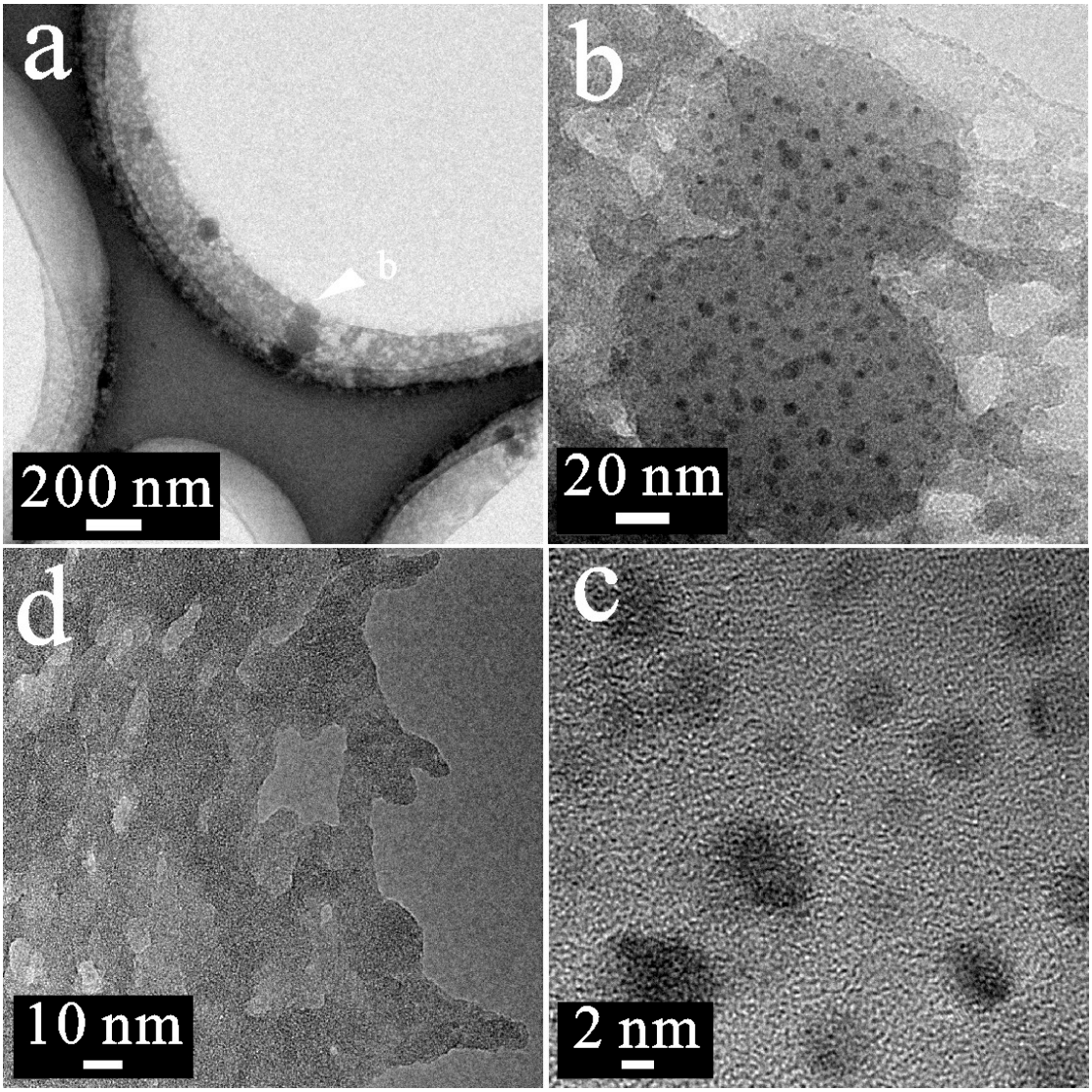

Figure S12. TEM images of objects formed in solution after 1 h reaction at 175 °C. c) HRTEM image of an aggregate of crystallites in (b), showing the difficulty in visualizing crystallites caused by surrounding of amorphous material produced from the aluminosilicate, TPA and NaOH precipitation during specimen drying, but it isn't difficult to confirm the MFI framework structure of the crystallites. d) Magnified view of a gel object in (a), indicating imprints after detachment of the polycrystal aggregates.

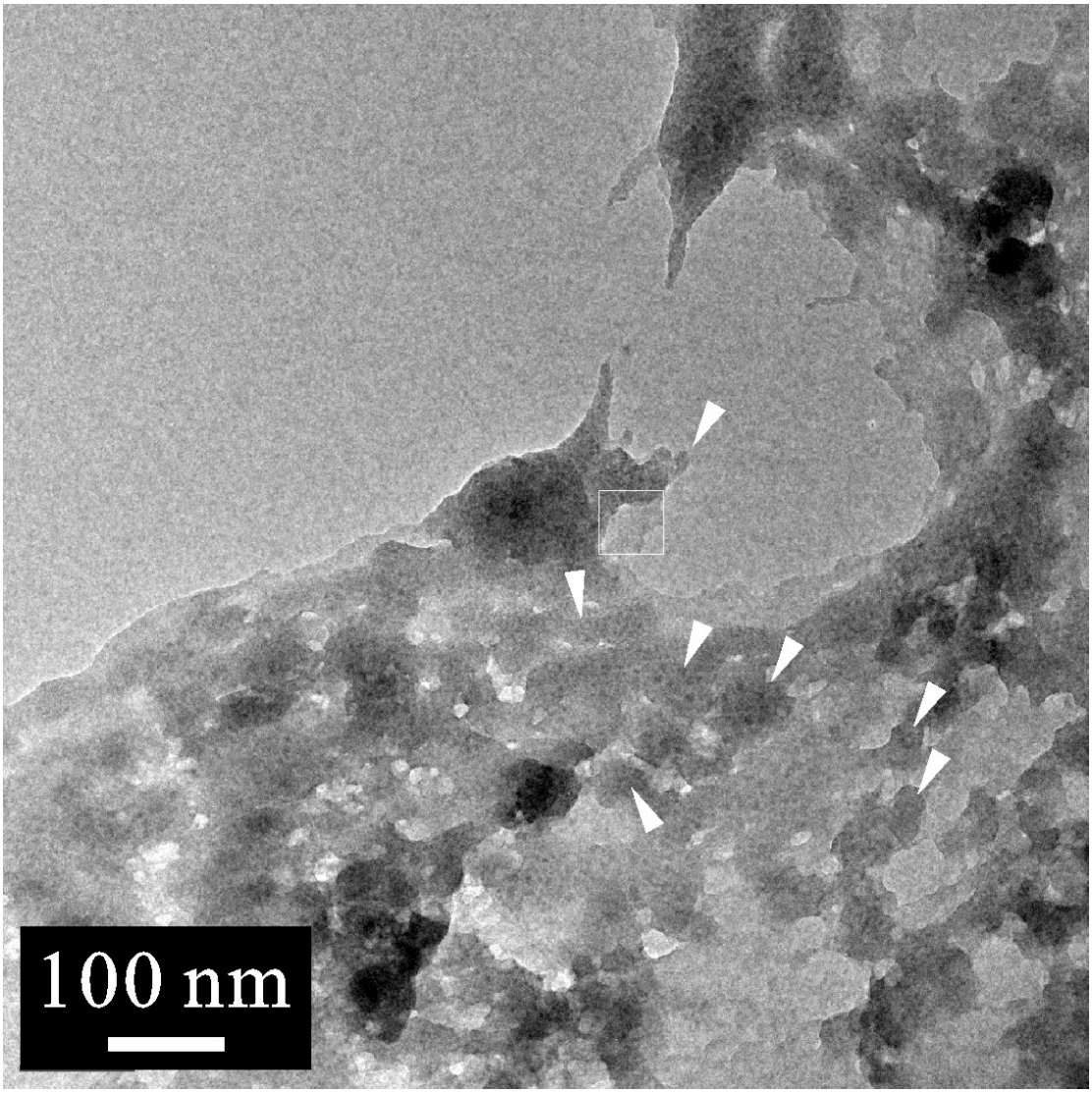

Figure S13. TEM image of the intermediate gel formed in solution after 30 min reaction at 175 °C. The arrowheads show aggregates of crystallites forming in the intermediate gel. The region marked by a square is shown magnified in Figure 5.

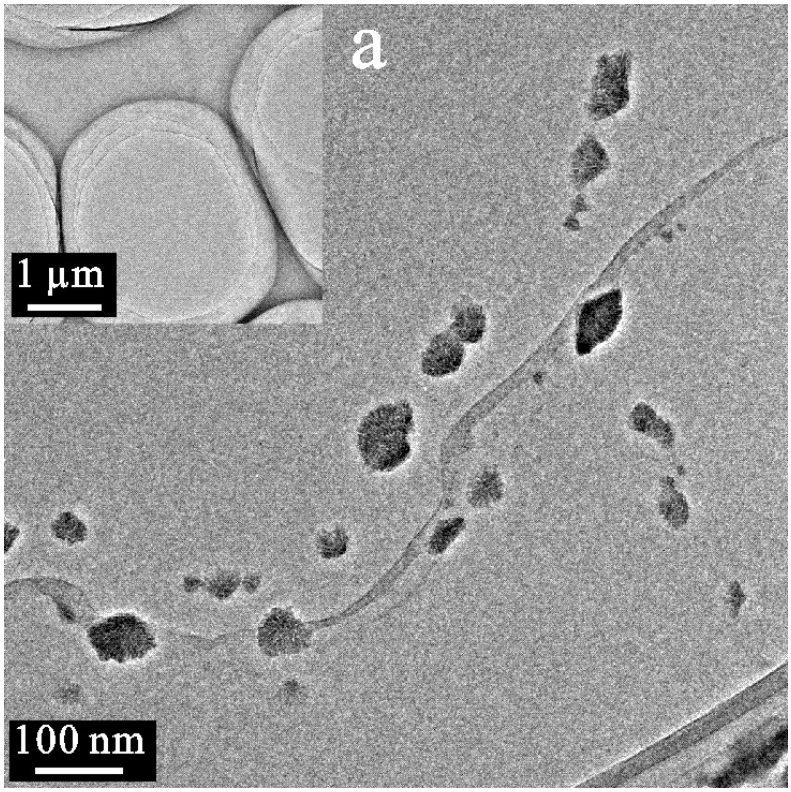

Figure S14. TEM images of aggregate particles derived from the extracted solution. Arrows in (b) highlight the 10-MR pores of the MFI framework which seem to exist in a tiny cluster. The curved white lines in (c) highlight the crystal perimeters of an aggregate-like crystal composed of ~1.5-nm-sized nuclei schematically shown in (e). (d) FFT of (c). (f) HRTEM of (b) showing an aggregate-like crystal. The first diffuse ring in FFT (inset) from the square region with d spacing about 1.0-1.1 nm, which can be the $d_{[200]}$ or $d_{[101]}$ of the MFI framework.

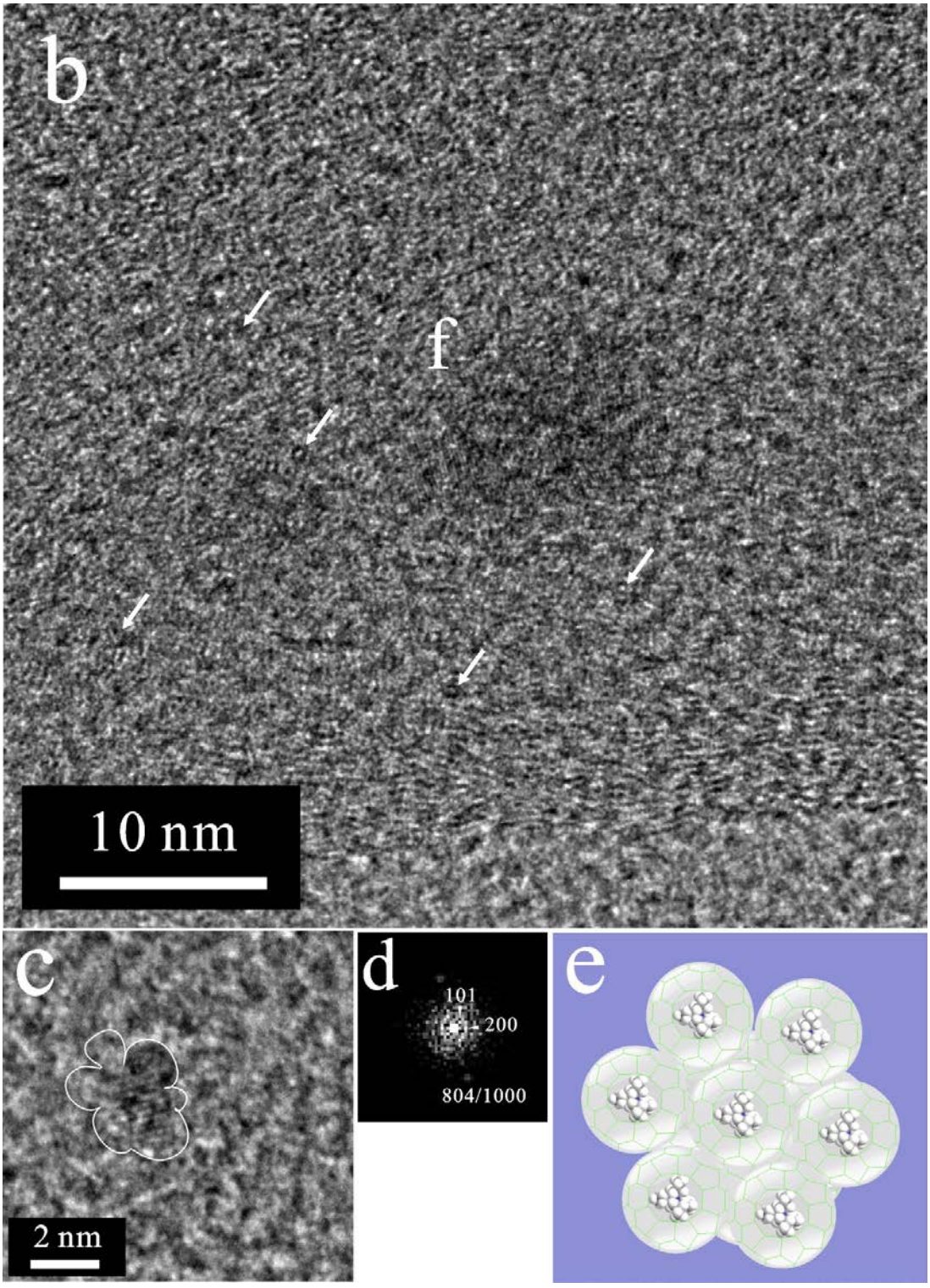

Figure S14

(Cont.)

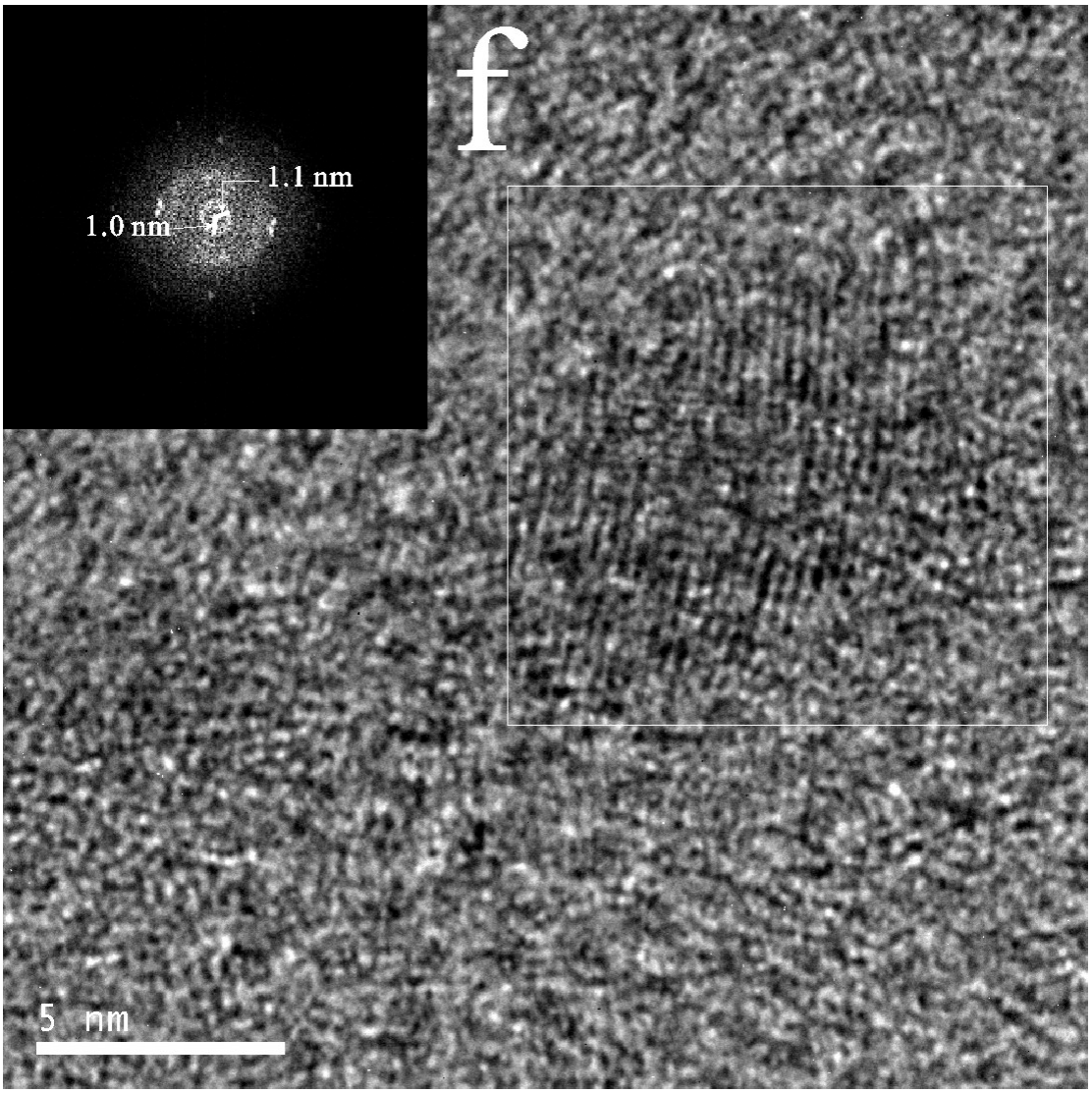

Figure S14

(Cont.)

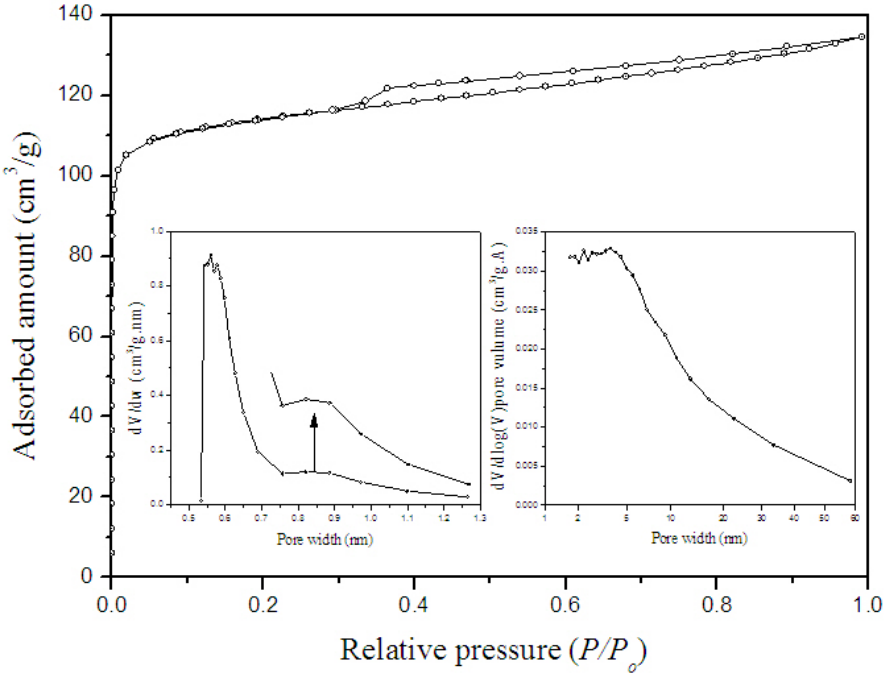

Figure S15. Argon adsorption–desorption isotherm of the hierarchically monolithic MFI zeolite obtained after 48 hours of the hydrothermal treatment at 175 °C. The micro-mesopore-size distributions are given in the insets. The presence of the microporous void with a broad peak centered at ~0.85 nm and mesoporous voids (2-50 nm) show the dissolution of T–O–T bonds that constitute the crystal lattice of the MFI framework.

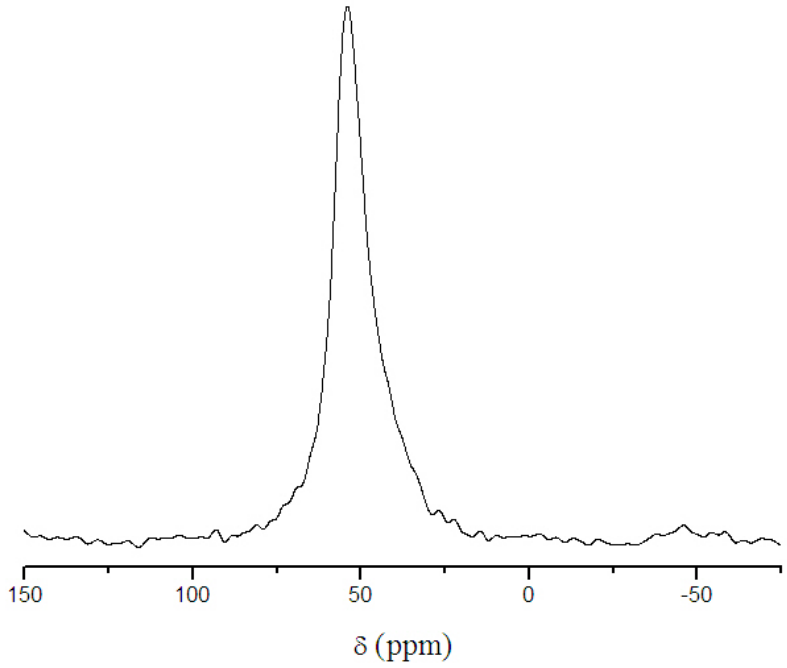

Figure S16. ^{27}Al NMR spectrum of the hierarchically monolithic MFI zeolite obtained after 48 hours of the hydrothermal treatment at 175 °C.

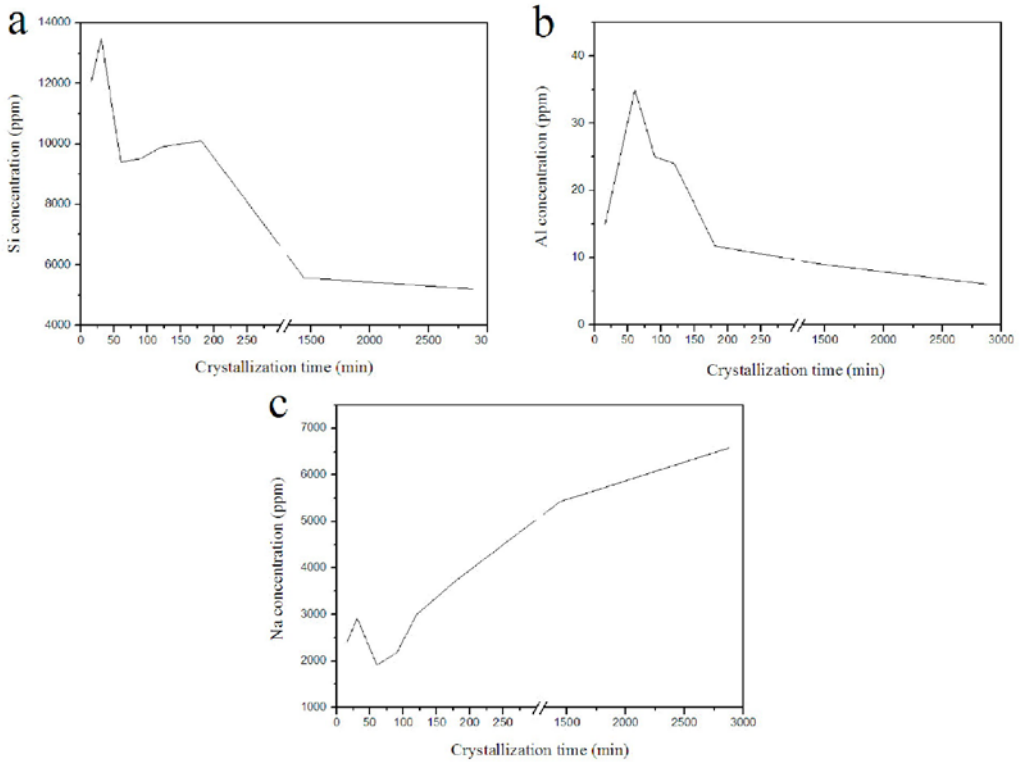

Figure S17. Concentration of (a) silicon, (b) aluminum and (c) sodium in the monolith-separated liquid phase obtained after various reaction times of the hydrothermal treatment at 175 °C.

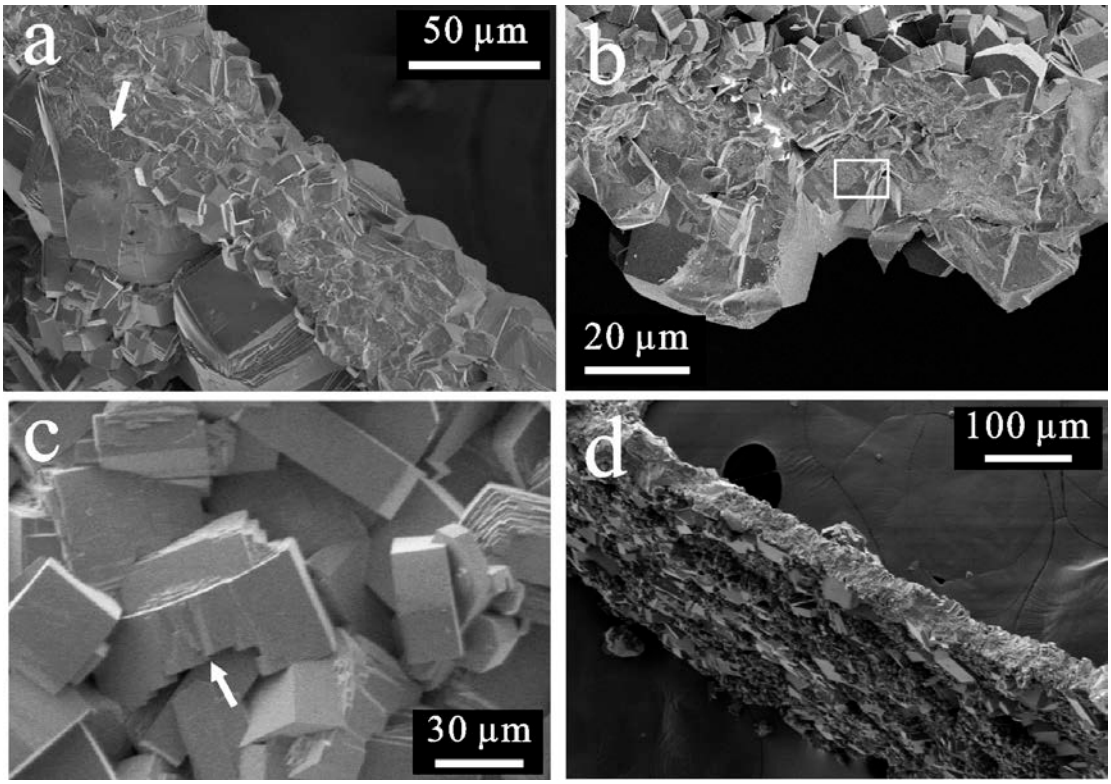

Figure S18. SEM images of samples after secondary crystallization of the liquid phase obtained after 30 min of the hydrothermal treatment at 175 °C for 24 hours (a-c) and 48 hours (d).